TRACE IMPULSIVE RESPONSE IN SOLAR FLARE FOOTPOINTS

T. Mrozek[1], S. Gburek[2], and M. Tomczak[1]

[1]Astronomical Institute, Wrocław University, ul. Kopernika 11, 51-622 Wrocław, Poland
[2]Space Research Centre, Polish Academy od Sciences, Solar Physics Division, ul. Kopernika 11, 51-622 Wrocław, Poland

ABSTRACT

We have analysed UV and EUV brightenings of flare footpoints during the impulsive phase using *TRACE* observations made in two filters: 171 and 1600 Å. *TRACE* 171 Å images have been desaturated using a method based on the diffraction pattern properties. Obtained observational characteristics of UV and EUV brightenings have been compared to those obtained for impulsive SXR brightenings seen in *Yohkoh*/SXT images. The quantitative analysis of fluxes for spatially resolved UV, EUV and HXR sources have been made and compared to results obtained for SXR sources. It has been found that the UV and EUV brightenings are produced by more energetic electrons than impulsive SXR brightenings.

Key words: Sun: corona - flares - X–rays, UV.

1. INTRODUCTION

The observations of the impulsive soft X-ray (SXR) brightenings offer a new diagnostic tool of the non-thermal electrons precipitation in solar flare footpoints. Impulsive SXR brightenings are caused mainly by non-thermal electrons with energies of 10-20 keV (Tomczak 1999, Mrozek and Tomczak 2004). More energetic electrons should reach the denser atmospheric layers (Farnik et al. 1997) and produce an impulsive reaction seen in the UV radiation.

Using a method developed for the impulsive SXR brightenings analysis (Tomczak 1999, Mrozek and Tomczak 2004) we investigated quantitatively several flare footpoints observed simultaneously by the HXT and *TRACE*.

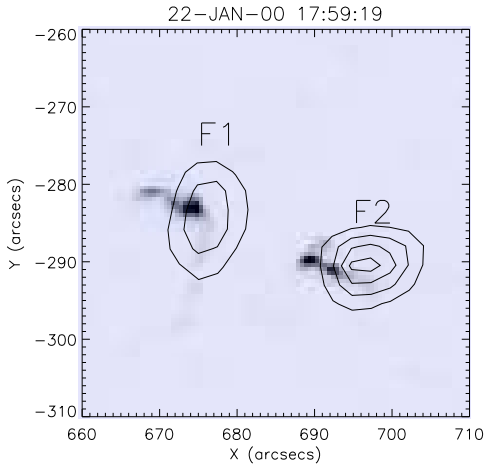

Figure 1. The image of the 22-Jan-00 flare obtained at the maximum of the HXR light curve. Grey scale represents the TRACE *(171 Å) emission distribution. Contours of the HXR emission are overplotted (30, 50, 70, 90% of the maximum intensity).*

2. ANALYSIS

Using the catalogue made by Nitta[1] we have chosen 13 flares which impulsive phases were well-observed by the HXT and *TRACE* in 171 Å (EUV) or 1600 Å (UV) filters. The list of selected flares is given in Table 1.

For further analysis we have chosen bright kernels of the UV or the EUV emission which were observed during the impulsive phase and were spatially related to HXR sources observed by the HXT. Usually UV and EUV emission regions were saturated. For *TRACE* observations in the 1600 Å filter we have found only four

[1]http://isass1.solar.isas.ac.jp/sxt_co/sxt_trace_flares/list.html

Table 1. List of investigated flares. (1) - number of event; (2) - date; (3) - GOES maximum time [UT]; (4) - GOES class; (5) - coordinates; (6) - observations in TRACE *171 Å; (7) - observations in* TRACE *1600 Å.*

(1)	(2)	(3)	(4)	(5)	(6)	(7)
1	18-JAN-99	08:04	M2.0	N21E09	+	-
2	22-JUN-99	18:29	M1.7	N23E39	+	-
3	19-SEP-99	23:12	C9.6	N21W76	+	-
4	22-JAN-00	18:01	M1.1	S21W49	+	-
5	08-FEB-00	09:00	M1.3	N25E26	+	-
6	15-MAR-00	03:42	C6.8	S17W13	-	+
7	15-MAR-00	05:43	C4.0	S18W14	-	+
8	15-MAR-00	18:40	M1.4	S17W22	-	+
9	18-MAR-00	21:02	M2.1	S12W64	+	+
10	23-MAY-00	20:53	C9.5	N20W42	+	-
11	25-JUL-00	02:49	M8.0	N04W07	+	-
12	12-APR-01	10:28	X2.1	S21W42	+	-
13	31-OCT-01	08:09	M3.2	N11E02	+	-

flares without saturation in footpoints during the impulsive phase. For *TRACE* observations in 171 Å filter we were capable of selecting larger data set - 10 flares. Signal in the saturated image portions were recovered using the diffraction pattern properties for 171 Å filter.

Lin et al. (2001) made a detailed analysis of the *TRACE* diffraction pattern and calculated how the signal in the diffraction structure of a given order is scaled relatively to the signal located at the zeroth order position.

Gburek et al. (2005) analysed the geometry of the *TRACE* diffraction pattern. In particular, it was shown there that structures seen in low diffraction orders are almost exact copies of the zeroth order structure scaled by a multiplicative constant and shifted by the appropriate translation vector. Hence, even if the signal at the zeroth order is saturated it still can be recovered from the signal observed in low diffraction orders.

We applied this observation for our selection of saturated *TRACE* 171 Å images. The signal in saturated pixels was determined by rescaling the signal from the most resolved, background subtracted diffraction structure seen in the first or the second order. An example of the signal distribution in saturated sources before and after the signal recovering is presented in Fig. 3.

For a further analysis we selected UV emission kernels which were correlated with HXR sources observed by the HXT. Typically, we observed several small kernels of UV emission which were correlated with one larger HXR source. For the flux comparision we integrated the signal from all UV kernels. Borders of the HXR source have been obtained using images reconstructed for all HXT channels and the time interval near the strongest HXR burst. Images have been reconstructed using the MEM-Sato (Sato et al. 1999) method.

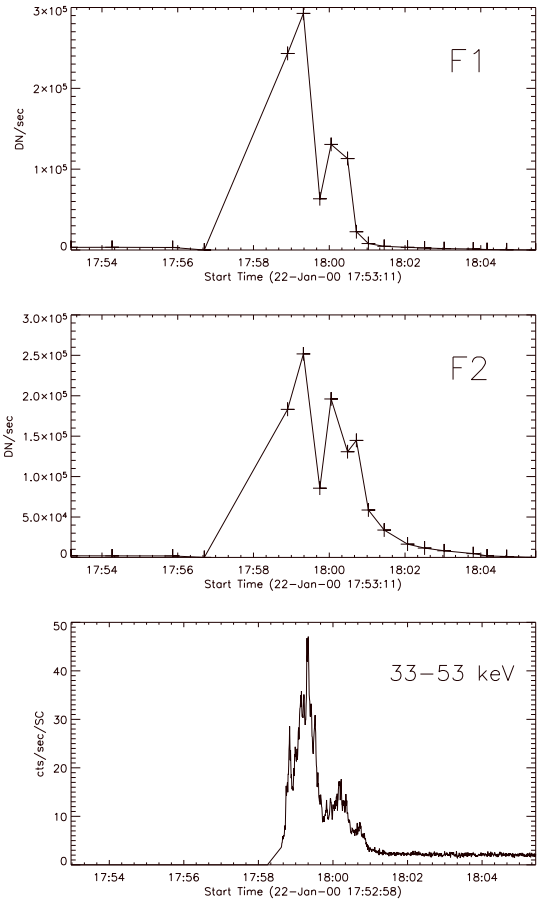

Figure 2. Top and middle panels - the TRACE 171 *Å light curves for the footpoints seen in Fig. 1. Bottom panel - the HXT (M2) light curve.*

3. RESULTS

In summary, we found 35 footpoints showing the impulsive UV (16 footpoints) or EUV (19 footpoints) brightenings and related to them HXR emission sources. The example of impulsive brightenings observed in the *TRACE* 171 Å is presented in Fig. 2. These footpoints come from 13 flares listed in Table 1. Figure 4 shows a relation between the HXR intensities obtained in the channel M1 and EUV (top panel) or UV (bottom panel) responses. In this figure values obtained for the complete events are marked by diamonds. As the complete event we considered the peak value of the HXR light curve and the total EUV or UV signal from all brightenings observed in that time in the flaring structure.

The correlation coefficients, $R = 0.52$ for EUV and $R = 0.67$ for UV, strongly support that these observables are a manifestation of a common physical phenomenon, namely non-thermal electron beams.

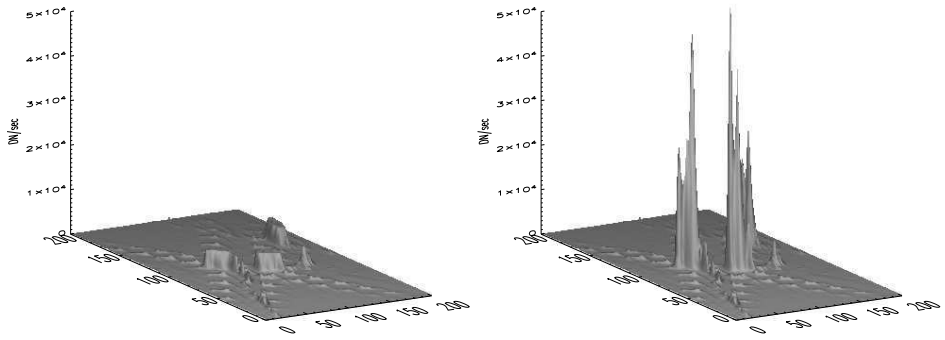

Figure 3. An example of desaturation in TRACE *171 Å. Left panel presents the signal distribution in an original image. In the right panel the signal has been recovered using diffraction pattern properties.*

Tomczak (1999) has defined the relative productivity of soft X-rays with regard to hard X-rays and showed that there is a clear relation between the relative productivity and the power-law index (γ) of the photon energy flux. He concluded that observed positive correlation between these observables proves that soft X-rays are produced mainly by the low energy electrons.

We defined the relative productivity of UV and EUV in similar way dividing EUV or UV response and the HXR emission for each source. The relation between the relative productivity and the power-law index is presented in Fig. 5. Mrozek and Tomczak (2004) calculated the correlation coefficient between the relative productivity of SXRs and γ for 31 footpoints. The obtained value, $R = 0.65$ (for M1 channel), is greater than values calculated for EUV ($R = 0.17$) and UV ($R = -0.40$). It can be connected with the height of the sources observed in footpoints in these three filters.

Each filter have a maximum response for different temperatures: 10^7 K for Al12, 10^6 K for the *TRACE* 171 Å and 10^4 K for the *TRACE* 1600 Å. Thus, using them we look at different levels of the solar atmosphere. In this paper we do not obtain absolute values of the height of the flux formation, but we can specify relative heights, i.e. which flux is produced higher or lower in the solar atmosphere. Assuming the following order down from the top: Al12, 171 Å, 1600 Å, we are able to explain different correlation coefficients obtained for these filters in terms of energy of non-thermal electrons depositing their energy at different levels.

For SXRs we found a high positive correlation coefficient between the relative productivity and γ. This means that the more energy is contained in low-energy electrons (a softer spectrum) the stronger heating in the low corona is observed. For a harder spectrum a relatively more energy is deposited in high energy electrons which are stopped in the low chromosphere. Thus, we observe clear anti-correlation for the relative productivity of UVs (*TRACE* 1600 Å).

Generally speaking, relations between fluxes measured in

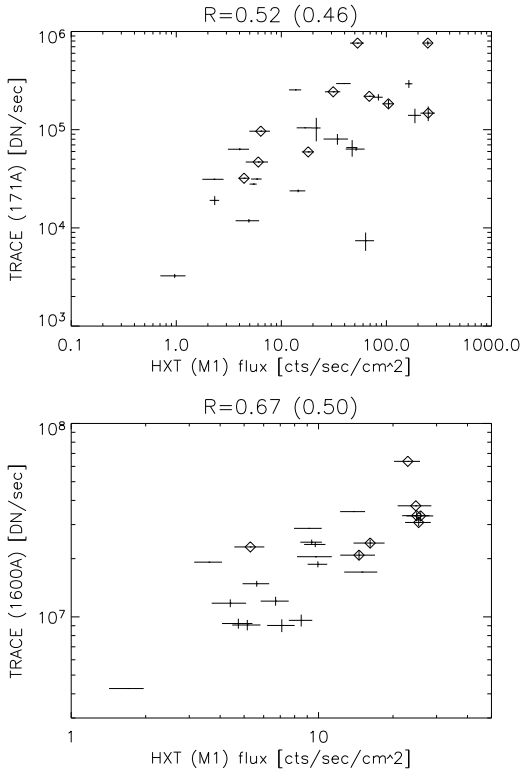

Figure 4. Relation between the thermal and non-thermal radiation observed in the HXT (M1) channel and TRACE *171 Å (top panel) and* TRACE *1600 Å (bottom panel). R is the correlation coefficient. Values for the complete events has been marked by diamonds. R for complete events is given in parenthesis.*

flare footpoints are a function of the energy of HXR photons. Using values obtained from the single power-law fit Mrozek and Tomczak (2004) calculated the HXR photon flux for each footpoint for different values of the energy. For each value of the energy they calculated a correlation

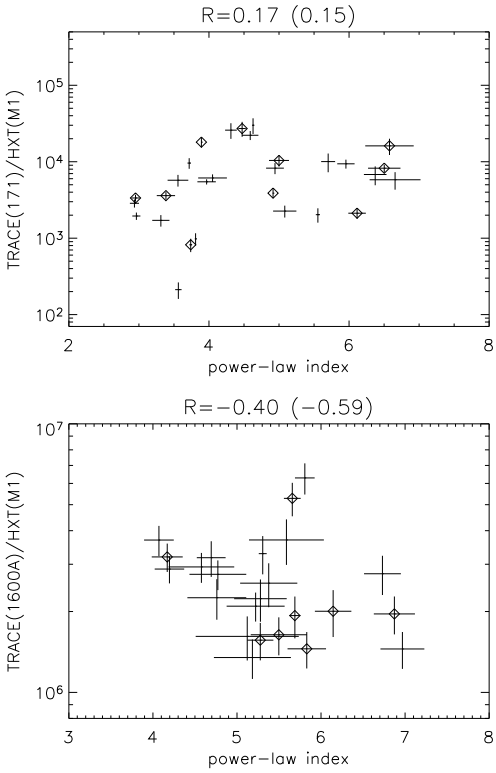

Figure 5. Plot of the relative productivity of EUVs (top panel) and UVs (bottom panel) with regard to hard X-rays HXT (M1) and power-law indexes taken from single power-law fit. R is the correlation coefficient. Values for the complete events has been marked by diamonds. R for complete events is given in parenthesis.

between the HXR photon flux and the SXR response and showed that the best correlation is for the range 12-15 keV. We calculated such correlations for EUV and UV responses. The result is presented in Fig. 6. For better presentation each curve has been shifted in the vertical direction to the same value since we are interested in the energy of the maxima. Again, it can be seen that there is a clear correlation between the thermal reaction in flare footpoint at some level and the energy of the HXR photons.

4. CONCLUSIONS

A generally good correlation between HXR intensities and UV or EUV responses strongly support that these observables are a manifestation of non-thermal electron beams.

A systematical change of the correlation coefficient between the relative productivity of SXRs, EUVs, and UVs with regard to HXRs and power-law index γ have been

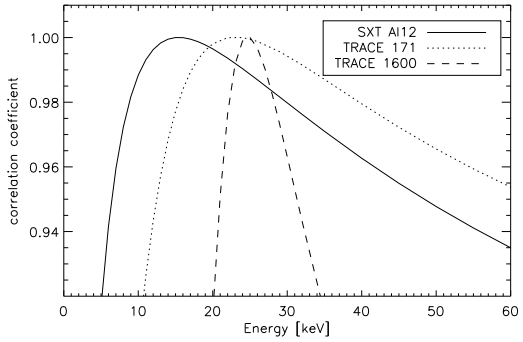

Figure 6. Correlation coefficient between the HXR flux and SXR, UV and EUV fluxes, respectively as a function of the photon energy [keV]. For better presentation each curve have been shifted vertically to the value of 1. Actual values of the maxima of correlation coefficients are: 0.75 (SXR), 0.52 (EUV) and 0.8 (UV).

found, i.e. from a strong positive for SXRs to anti-correlation for UVs. We found that such a trend can be explained in terms of the height in footpoints and the energy of the non-thermal electron beam.

For each footpoint we calculated the HXR photon flux for different values of the energy and calculated the correlation coefficient between these and EUV or UV emissions. Comparing this with the result obtained for the relative productivity of SXRs (Mrozek and Tomczak 2004) we found the systemic trend: the thermal reaction at a particular level depends on the energy of non-thermal electrons depositing their energy at this level.

ACKNOWLEDGEMENTS

The *Yohkoh* satellite was a project of the Institute of Space and Astronautical Science of Japan. The *TRACE* satellite is a NASA Small Explorer (SMEX) mission. This investigation has been supported by grant No. 2P03D 001 23 from the Polish Commitee for Scientific Research (KBN).

REFERENCES

Farnik, F., Hudson, H., & Watanabe, T. 1997, *A&A*, 320, 620
Gburek, S., Sylwester, J., Mrozek, T., 2005, this issue
Lin, A.C., Nightingale, R.W., Tarbell, T.D. 2001, *Sol. Phys.*, 198, 385
Mrozek, T., & Tomczak, M. 2004, *A&A*, 415, 377
Sato, J., Kosugi, T., & Makishima, K. 1999, *Publ. Astron. Soc. Japan*, 51, 127
Tomczak, M. 1999, *A&A*, 342, 583